

# Effect of Yb Doping on the Afterglow and Thermoluminescent Properties of ZnO Nanophosphors

U. Pal<sup>1</sup>, R. Meléndrez<sup>2</sup>, V. Chernov<sup>2</sup>, and M. Barboza-Flores<sup>2,\*</sup>

<sup>1</sup>Instituto Física, Universidad Autónoma de Puebla, Apartado Postal J-48, Puebla, 72570 México

<sup>2</sup>Centro de Investigación en Física, Universidad de Sonora, Apartado Postal 5-088, Hermosillo, Sonora, 83190 México

ZnO nanophosphors prepared by a glycol mediated chemical synthesis exhibit afterglow (AG) and thermoluminescence (TL) after excitation with beta rays. These properties, which are of great interest in dose assessment of ionizing radiation fields, could be appreciably modified by Yb doping. Concentration of 1, 2 and 5% diminished the AG and TL efficiency and modified the TL glow curve shape significantly. However, the 5% Yb doping concentration reduced the AG and TL fading behavior, improving the use of ZnO:Yb (5%) as potential TL ionizing radiation dosimeter.

**Keywords:** Thermoluminescence, Afterglow, ZnO:Yb Nanocrystals, Phosphors.

## 1. INTRODUCTION

Special characteristics of nanostructured materials open up the possibility for their applications in several fields including optoelectronic devices<sup>1,2</sup> and biological sensors.<sup>3,4</sup> However, their luminescence properties seem to depend strongly on the synthesis technique, particle size and surface morphology. Furthermore, in the case of nanostructured ZnO, the overall photoluminescence (PL) properties depend on the defects involved in the radiative recombination processes responsible for the observed light emission.<sup>5,6</sup>

Thermoluminescence (TL) is a phenomenon associated to the thermally stimulated light emission after a material sample is exposed to a beam of ionizing radiation or UV light. The incident radiation creates free electrons and holes, of which some are trapped at localized trap sites inside the band gap. Those stable trapped charges may remain there until detrapping is produced by thermal stimulation. Thermal stimulation causes the charge carriers to leave the localized trap states and to move either to the valence (holes) or conduction (electrons) bands, until they recombine with opposite charge centers, emitting light. A highly efficient TL material allows the dose assessment of the incident radiation beam, which is of extreme importance in medical and clinical applications like radiotherapy. Radiation oncology and radiotherapy is one of the fields in which more adequate and efficient dose determination is highly required, and a dosimeter with real-time and

*in-situ* dose evaluation possibilities will be greatly beneficial for the patients undergoing radiation treatments. Having a nanostructured dosimetric material with high charge electron-hole pair creation efficiency, good sensitivity, low fading, adequate energy response and reproducibility would be extremely beneficial to dose evaluation in well-localized tissues or specific zones of human body. Nanostructured materials are finding important application in medicine through exploiting its luminescent, non-linear optical and radiation dose enhancement properties. It is pertinent just to mention the use of gold nanoparticles as dose enhancer and the promising results in tumor radiotherapy in mice.<sup>7,8</sup> This justifies pursuing the research of new materials on the nanometric scale capable of enhancing the safety of radiation treatments in medical physics as compared to those of traditional dosimeter protocols.

In this article, we present results on the TL properties of undoped and Yb doped ZnO nanophosphors and their dependence on doping concentration, as part of a systematic study on the investigation of nanostructured materials with potential application as radiation dosimeters.<sup>9,10</sup> It is found that the TL properties of ZnO:Yb nanophosphors exposed to beta radiation are strongly dependent on the Yb concentration. The Yb (5%) doping diminishes the TL efficiency but it generates a more thermally stable TL glow peak as compared to pure ZnO.

## 2. EXPERIMENTAL DETAILS

The undoped and doped ZnO nanostructures were prepared through a glycol mediated chemical synthesis using a

\*Author to whom correspondence should be addressed.

mixture of anhydrous zinc acetate  $[(C_2H_3O_2)_2Zn]$ , Aldrich, 99.99% and ethyleneglycol (Baker) and heating at 440 K temperature for 2 h. The details of synthesis procedure are discussed elsewhere.<sup>9</sup> Morphology of the doped and undoped samples was studied using a JEOL JSM LV 5600 scanning electron microscope with a Noran SuprDry analytical system attached. Crystalline quality of the samples was studied by recording their X-ray diffraction (XRD) spectra in a Phillips X'Pert diffractometer using  $CuK\alpha$  radiation ( $\lambda = 1.5406 \text{ \AA}$ ). The TL

measurements were performed using a Risø TL/OSL System (model TL-DA-15). Beta irradiation exposures to the samples were performed using a  $^{90}Sr$ - $^{90}Y$  source having an activity of 0.04 Ci and 5 Gy/min dose rate. The heating rate for TL readouts was 5 K/s.

### 3. RESULTS AND DISCUSSION

Spherical shaped ZnO particles of sizes ranging 130–1200 nm were synthesized. In general, the average

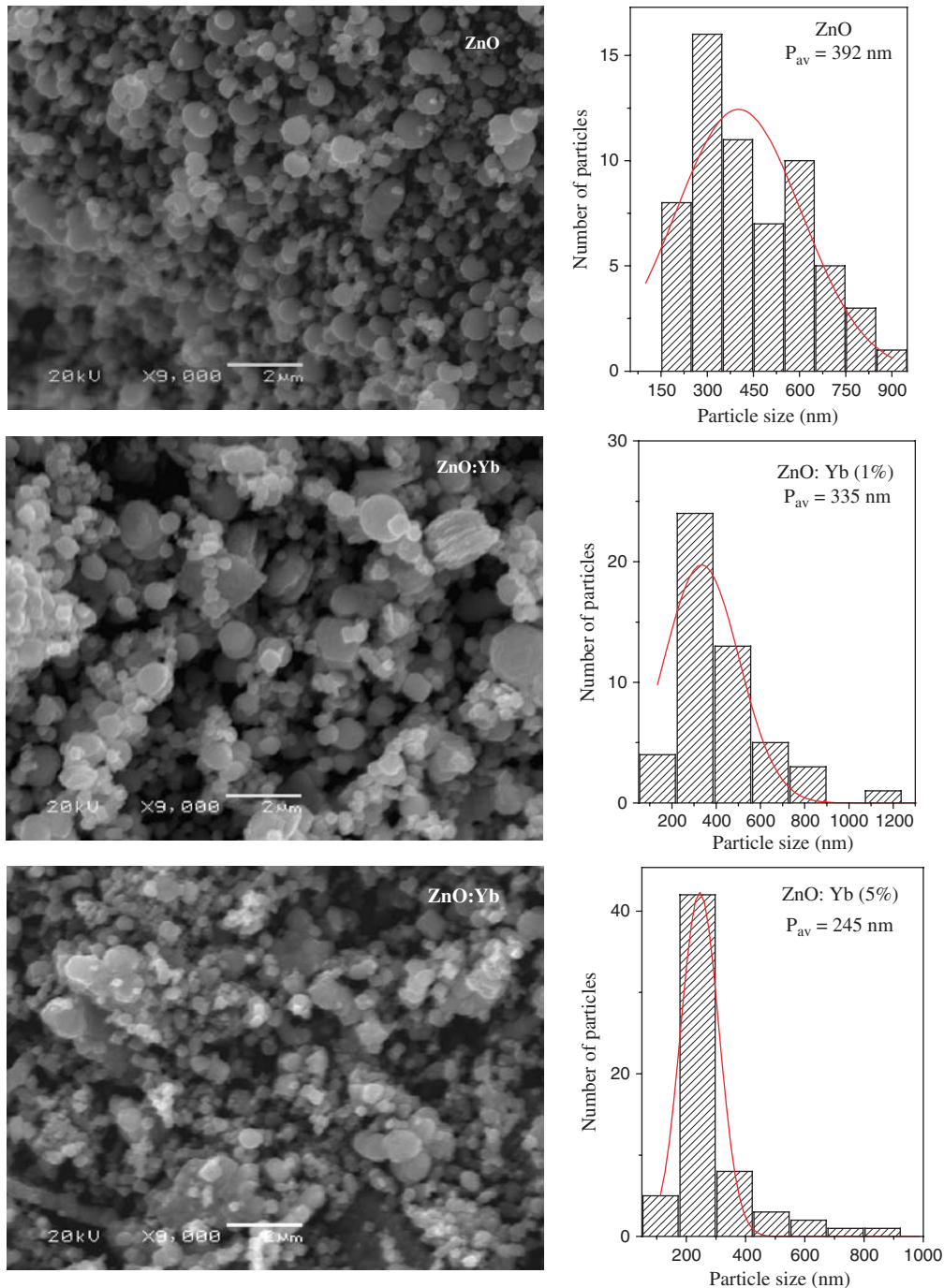


**Fig. 1.** Typical SEM micrographs and corresponding particle size distribution histograms for the undoped and Yb doped ZnO nanostructures.

**Table I.** EDS composition analysis of the doped and undoped ZnO nanostructures.

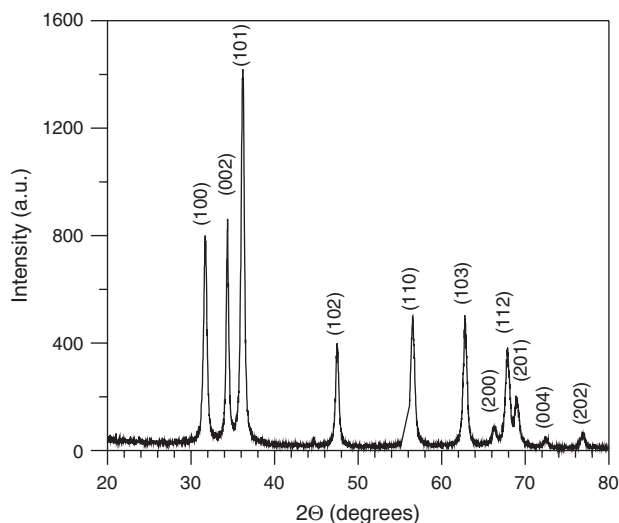
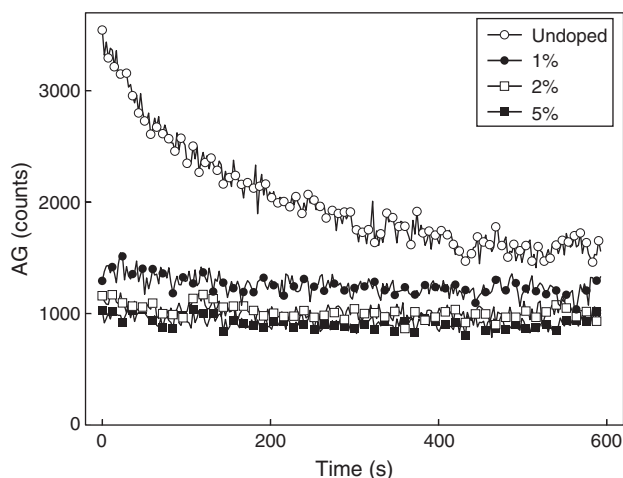
Sample	Zn (at.%)	O (at.%)	Yb (at.%)
ZnO	44.80	55.20	0.0
ZnO:Yb (1%)	44.00	55.50	0.50
ZnO:Yb (2%)	43.85	55.50	0.65
ZnO:Yb (5%)	43.70	55.50	0.80

size of the particles decreased with the increase of Yb doping concentration. In the Figure 1, the SEM micrographs and particle size distributions of the samples are presented. From the size distribution histograms, we can observe that the average size of the particles varied from 392 nm for undoped to 245 nm for 5% Yb doped ZnO.

EDS spectra of the samples did not reveal any other emission peak except of Zn, O and Yb, indicating the absence of any other impurities in the samples. In the Table I, estimated atom % of the constituents in the samples is presented. It must be observed that though we doped the samples with 1, 2 and 5 nominal % of Yb, only 0.5, 0.65 and 0.8 atom % of Yb were incorporated, respectively, in ZnO.

All the samples revealed similar XRD patterns of crystalline ZnO in hexagonal wurtzite phase (Fig. 2). XRD patterns of the doped samples are very similar to the undoped one, revealing no Yb related peak or its oxide.

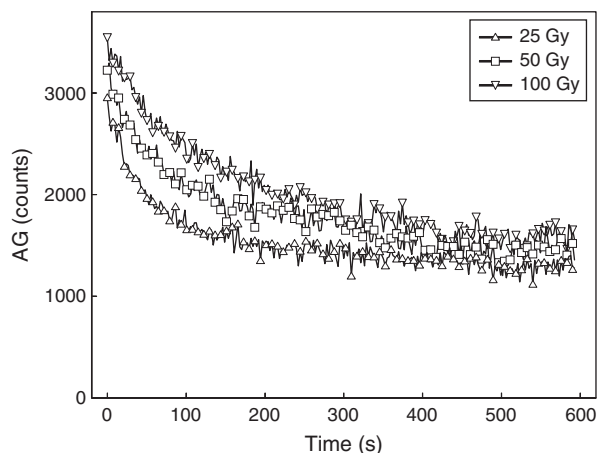
The ZnO:Yb nanophosphors exhibited a characteristic afterglow (AG) luminescence immediately after beta ray irradiation as indicated in Figure 3. The AG signal displays a typical decay behavior and comes from the radiative recombination of some of the charge carriers detrapped by room temperature instabilities. AG is an unwanted feature if dose assessment is the purpose, since this type of recombination is associated to electrons and holes produced by irradiation exposure and are not stably trapped at localized

**Fig. 2.** XRD pattern of the undoped ZnO nanostructures prepared by glycol mediated synthesis.**Fig. 3.** Room temperature afterglow decay behavior of ZnO:Yb after irradiation with 100 Gy beta ray dose as a function of Yb concentration.

trapping states. Therefore, due to AG recombination, the measured dose will not account for the charge carriers detrapped and recombined as AG luminescence. The AG is stronger for pure ZnO as compared to ZnO:Yb (1%) to become almost equal to background noise signal for ZnO:Yb (5%). Then evidently the 5% Yb concentration reduces almost to zero the AG emission.

As the beta ray dose increases, the AG intensity also increases as shown in Figure 4 for the undoped ZnO sample, although the typical time decay feature is maintained, perhaps as a consequence that the characteristic trapping and detrapping probabilities cross sections remains the same irrespective of the irradiation dose.

Due to the observed AG, it was necessary to use an adequate delay time after irradiation in order to proceed with the TL read out process. Figure 5 illustrates the TL glow curve of ZnO:Yb as a function Yb concentration after irradiating with 100 Gy beta ray dose. The undoped ZnO specimen shows the highest TL efficiency

**Fig. 4.** Room temperature AG decay curves of nanostructured undoped ZnO as a function of beta ray irradiation dose.

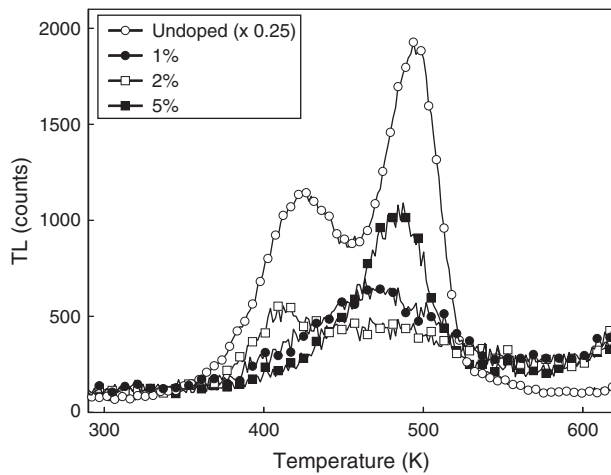


**Fig. 5.** Relative comparison of TL glow curves of ZnO:Yb samples as a function of Yb concentration exposed at room temperature to a 100 Gy beta ray dose.

than those containing 1, 2, and 5% Yb concentration. However, there is no systematic behavior with doping concentration since TL efficiency and glow curve shape are severely affected by Yb concentration. The striking feature is the single TL glow peak peaked at 483 K displayed by ZnO:Yb (5%) compared to the two main TL glow peaks for the other ZnO:Yb samples. The changes in the TL glow curve shapes means that the Yb doping causes a major effect on the charge trapping processes taking place in the nanophosphor material after irradiation. The measured quenching effects on the AG and TL response in ZnO:Yb as compared to thermoluminescent ZnO, may be due to the radiation losses caused by the metallic Yb atoms as beta electrons passes through the ZnO:Yb nanostructure. The radiation losses means less local radiation dose on ZnO phosphor which results in lower AG and TL response. The distinctive nature of the trapping cross section probabilities for the localized trap states is shown in Figure 6,

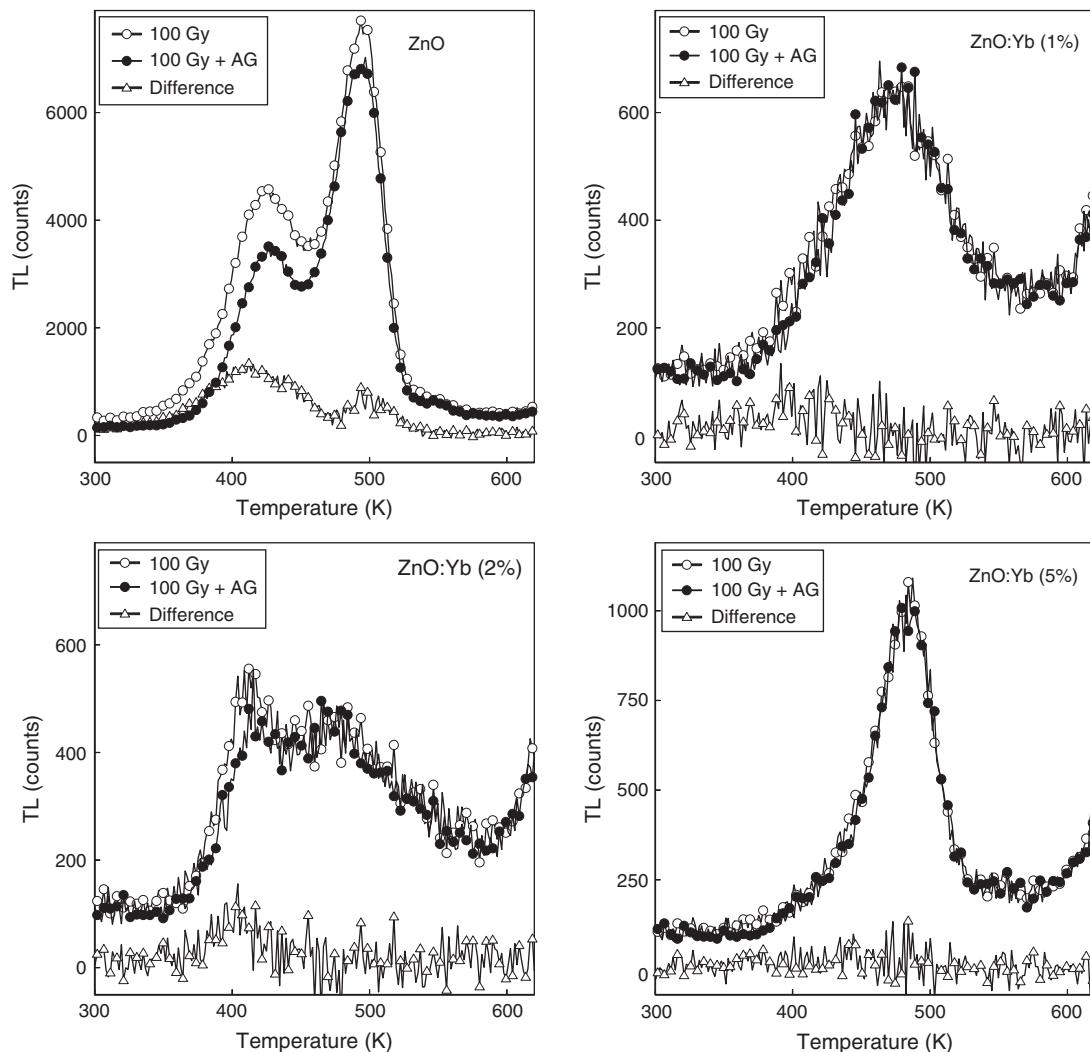


**Fig. 6.** Comparison of the TL glow curves exposed to a beta ray dose of 100 Gy and taken before and after the AG measurement of nanostructured undoped and doped with Yb ZnO. The triangles are the difference TL curves showing effect of AG readout.

which shows the TL glow curves taken before and after the AG measurements in sample at 100 Gy of beta ray irradiation. It is observed that a major charge detrapping process occurs for the localized trap states at the lower temperature side of the glow curve for undoped, 1 and 2% Yb doping ZnO, being almost inexistent in ZnO:Yb (5%). It is pertinent to call the attention upon that the room temperature depletion of the sample TL glow curve after irradiation is called thermal fading. It may be also noticed from Figure 6 that not only the glow peak intensity or glow curve shape changes but the width of the peaks also changes. It provides an indication that the TL kinetics of ZnO may also varies with the Yb doping concentration. A careful examination of these changes was made by a computer glow curve deconvolution procedure for all the Yb concentrations used. The kinetic processes involved in the TL of the nanostructured ZnO phosphors were extracted by using a deconvolution computer fitting

program based on the non-linear least-square Marquardt fitting method.<sup>11,12</sup> The program was capable of processing several overlapped TL glow peaks simultaneously to evaluate their kinetic parameters. The TL glow peaks were fitted to the first and second order kinetics.<sup>13</sup> The equations describing the emptying of the filled TL traps were written as follows:

$$S(T) = S_0 \exp \left[ -\frac{sk_B T^2}{\beta E} \exp \left( -\frac{E}{k_B T} \right) \left( 1 - \frac{2k_B T}{E} \right) \right] \quad (1)$$

$$S(T) = S_0 \left[ 1 + \frac{sk_B T^2}{\beta E} \exp \left( -\frac{E}{k_B T} \right) \left( 1 - \frac{2k_B T}{E} \right) \right]^{-1} \quad (2)$$

Here,  $S(T)$  represents the total light emitted during heating from temperature  $T$  up to a full emptying of the TL traps, which is proportional to the current concentration of filled traps. The TL signal  $\Delta S(T)$  of the Risø TL/OSL system is

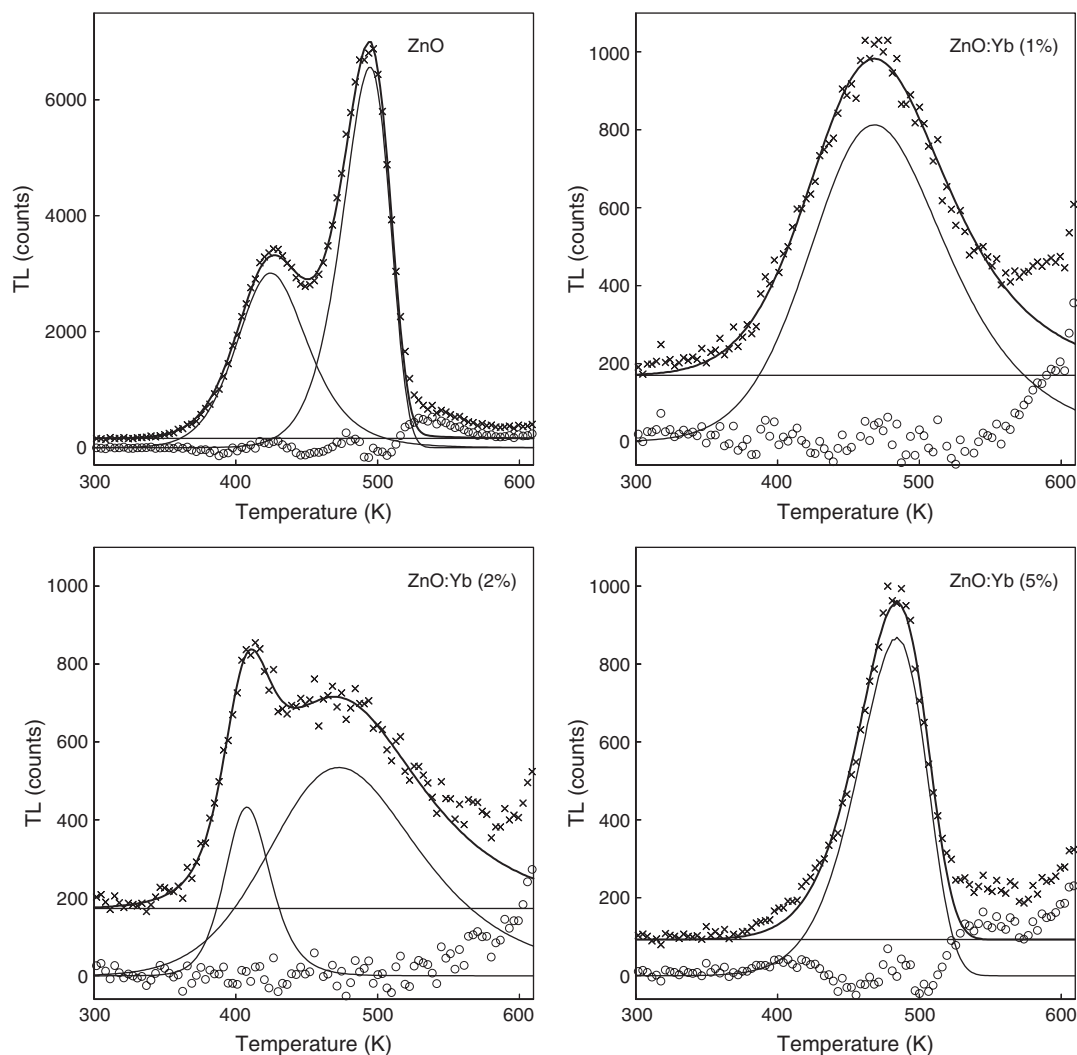


**Fig. 7.** Computer deconvolution of TL glow curves for undoped ZnO and ZnO doped with 1, 2 and 5% Yb exposed to 100 Gy of beta radiation. The crosses are the experimental TL data, thin lines are the deconvoluted TL peaks and background, the bold line is the sum of the separate peaks and background, the circles are the residuals of the fitting process. The kinetic parameters of the separate peaks are presented in Table II.

**Table II.** Kinetic parameters of TL glow peaks for undoped and doped with Yb ZnO nanostructures.

Sample	Peak maximum (K)	Kinetics order	Activation energy (eV)	Frequency factor (1/s)
ZnO	423	2	0.79	$7 \times 10^8$
	495	1	1.23	$1 \times 10^{12}$
ZnO:Yb (1%)	471	2	0.51	$3 \times 10^4$
ZnO:Yb (2%)	408	2	1.27	$2 \times 10^{15}$
	476	2	0.47	$1 \times 10^4$
ZnO:Yb (5%)	483	1	0.80	$4 \times 10^7$

proportional to some amount of light emitted during heating from temperature  $T$  to  $T + \Delta T$  and can be presented as  $\Delta S(T) = S(T) - S(T + \Delta T)$ ,  $S_0$  is the total TL signal emitted during the heating process (the peak area).  $E$  (eV) is the activation energy of the TL trap,  $s$  ( $s^{-1}$ ) is the frequency factor for first order and the effective frequency factor for second order kinetics (proportional to the frequency factor of the TL trap with the proportional coefficient depending on TL model used to derive the glow curve shape),  $\beta$  ( $Ks^{-1}$ ) is the heating rate and  $k_B$  is the Boltzmann's constant.

The computer deconvolution results are shown in Figure 7, which displays the experimental TL data along with the deconvoluted TL glow peak components (thin lines) and the residuals of the fitting process. The fittings clearly show the changes in TL kinetics produced by Yb doping. Table II provides the evaluated kinetic parameters. The TL spectra of ZnO:Yb (5%) and ZnO:Yb (1%) are composed of a single first and second order kinetic peaks, respectively, while the ZnO:Yb (2%) has two second order kinetics peaks. The undoped ZnO is fitted well with two TL glow, first and second order kinetic peaks.

It should be mentioned that for strongly overlapped peaks, the deconvolution is ambiguous and several combinations of TL peak parameters can fit a glow curve with more or less equal precision. The calculated kinetics values shown in Table II must be considered as approximate values. They were obtained by having the best fit to the experimental data using a specific form for the first and second order kinetics processes given by Eqs. (1 and 2). Therefore, additional investigation about the trap parameters of the TL peaks in nanostructured ZnO:Yb is required.

## 4. CONCLUDING REMARKS

The Yb doping in ZnO nanophosphors affects its TL glow curve shape, TL kinetic parameters, as well as TL efficiency. Those parameters also depend on the Yb doping concentration. Such effects are very important in pursuing applications of nanostructured ZnO:Yb in radiation thermoluminescence dosimetry. However, the Yb doping strongly reduces the AG of ZnO nanophosphors. A nonophosphor suitable for TL dose assessment should have a high TL efficiency as well as low AG and thermal fading. These aspects are closely related to the phosphor synthesis as well as the different intrinsic defects produced by the synthesis process and should be the matters of further investigation.

**Acknowledgments:** We acknowledge UC-MEXUS and CONACyT, Mexico for their financial supports through Grants # CN-05-215 and # 46269 respectively.

## References and Notes

1. S. Nakamura, M. Senoh, S. Nagahama, N. Iwasa, T. Yamada, T. Matsushita, Y. Sugimoto, and H. Kiyoku, *Appl. Phys. Lett.* 69, 1477 (1996).
2. F. H. Nicoll, *Appl. Phys. Lett.* 9, 13 (1996).
3. J. S. Kim, W. Park, C. Lee, and G. Yi, *J. Korean Phys. Soc.* 49, 1635 (2006).
4. N. Kumar, A. Dorfman, and J. Hahm, *Nanotechnol.* 17, 2875 (2006).
5. A. B. Djurišić, Y. H. Leung, K. H. Tam, L. Ding, W. K. Ge, H. Y. Chen, and S. Gwo, *Appl. Phys. Lett.* 88, 103107 (2006).
6. A. F. Vladimir, A. A. Khan, A. B. Alexander, X. Faxian, and L. Jianlin, *Phys. Rev. B* 73, 165317 (2006).
7. J. F. Hainfeld, D. N. Slatkin, and H. M. Smilowitz, *Phys. Med. Biol.* 49, N309 (2004).
8. S. H. Cho, *Phys. Med. Biol.* 50, N163 (2005).
9. U. Pal, R. Meléndrez, V. Chernov, and M. Barboza-Flores, *Appl. Phys. Lett.* 89, 183118 (2006).
10. E. De la Rosa, R. A. Rodríguez, R. Meléndrez, P. Salas, L. A. Diaz-Torres, and M. Barboza-Flores, *Nucl. Instr. Meth. B* 255, 357 (2007).
11. P. R. Bevington, *Data Reduction and Error Analysis for the Physical Sciences*, McGraw-Hill, New York (1969), Chap. 11.
12. W. H. Press, B. P. Flannery, S. A. Teukolsky, and W. T. Vetterling, *Numerical Recipes*, Cambridge University Press, Cambridge (1986), Chap. 14, pp. 523–528.
13. R. Chen and S. W. S. McKeever, *Theory of Thermoluminescence and Related Phenomena*, World Scientific, Singapore (1997), Chap. 2, pp. 29–31.

Received: 7 December 2006. Accepted: 11 June 2007.